

SUPPORTING INFORMATION

Spectroscopic Evidence and Density Functional Theory (DFT) Analysis of Low Temperature Oxidation of Cu^+ to $\text{Cu}^{2+}\text{NO}_x$ in Cu-CHA Catalysts: Implications for the SCR- NO_x Reaction Mechanism

Marta Moreno-González,^{†, ‡} Reisel Millán,[†] Patricia Concepción, Teresa Blasco^{} and Mercedes Boronat^{*}*

Instituto de Tecnología Química, Universitat Politècnica de València - Consejo Superior de Investigaciones Científicas, Av. de los Naranjos, s/n, 46022 Valencia, Spain

[‡]Present address: Department of Chemistry, The University of British Columbia, 2036 Main Mall, Vancouver, British Columbia V6H1Z1, Canada

COMPUTATIONAL DETAILS.

Calculation of Gibbs free energies.

The absolute Gibbs free energies of all species (minima and transition states) are given by:

$$G = E_{\text{tot}} + E_{\text{zpe}} + E_{\text{vib}} - TS_{\text{vib}}$$

where E_{tot} is the electronic energy obtained from the DFT calculation, E_{zpe} is the zero point energy correction, E_{vib} is the vibrational thermal energy contribution and S_{vib} is the vibrational entropy. The vibrational contributions to the energy and entropy were calculated according to:

$$E_{\text{zpe}} = \sum_{i=1}^{3N-6} \frac{1}{2} h\nu_i$$
$$E_{\text{vib}} = R \sum_{i=1}^{3N-6} \frac{h\nu_i}{k_B(e^{h\nu_i/k_BT} - 1)}$$
$$S_{\text{vib}} = R \sum_{i=1}^{3N-6} \left[\frac{h\nu_i}{k_BT(e^{h\nu_i/k_BT} - 1)} - \ln(1 - e^{h\nu_i/k_BT}) \right]$$

using the vibrational frequencies ν obtained from the DFT calculations. In the case of gaseous molecules the rotation and translational contributions to the entropy and energy were also included in the calculation of the free energy as follows:

$$G = E_{\text{tot}} + E_{\text{zpe}} + E_{\text{vib}} + E_{\text{rot}} + E_{\text{trans}} - T(S_{\text{vib}} + S_{\text{rot}} + S_{\text{trans}})$$

The rotational corrections (E_{rot} , S_{rot} , E_{trans} ,) were calculated using the Gaussian09 package.¹ The translational correction of the entropy S_{trans} is given by:

$$S_{\text{trans}} = R \left\{ \ln \left[\left(\frac{2\pi M k_B T}{h^2} \right)^{3/2} V \right] + \frac{3}{2} \right\}$$

For the processes of adsorption of the reactant molecules on the copper active sites we considered that the gas phase molecules are already confined within the channel system of the catalyst, so that they can only move within the free volume inside the unit cell which is 17% in the case of the CHA structure.² All equations used so far were taken from reference 3.

The Gibbs free energies of adsorption ΔG_{ads} were calculated as:

$$\Delta G_{\text{ads}} = G_{\text{structure}} - G_{\text{Cu-CHA}} - G_{\text{molecule}}$$

where $G_{\text{structure}}$ is the Gibbs free energy of the structure with the adsorbed molecule, $G_{\text{Cu-CHA}}$ is the free energy of the CHA catalyst and G_{molecule} is the Gibbs free energy of the molecule in gas phase.

The Gibbs free energies of activation ΔG_{act} and reaction ΔG_{reac} were calculated as:

$$\Delta G_{\text{act}} = G_{\text{TS}} - G_{\text{R}}$$

$$\Delta G_{\text{reac}} = G_{\text{P}} - G_{\text{R}}$$

where G_{R} is the free energy of the reactant R, G_{TS} is the free energy of the transition state and G_{P} is the free energy of the product P.

TABLES

Table S1. Chemical composition of Cu-CHA catalysts prepared by one-pot synthesis.

Catalyst	Si/Al	(P+Al)/Si	Cu/Al	Cu/Si	wt% Cu
Cu-SSZ-13	8.8	-	0.58	-	4.9
Cu-SAPO-34	-	8.1	-	0.5	3.9

Table S2. EPR parameters of signal $\text{Cu}^{2+}_{\text{SII}}$ of the dehydrated Cu-SSZ-13 zeolite in spectra recorded at different temperatures (T_m).

	$T_m/^\circ\text{C}$	A_{II}/G	g_{II}
Cu-SSZ-13	-170	151	2.347
	25	143	2.355
	170	137	2.361
	230	134	2.363

Table S3. Relative stability (in kcal/mol) of different distributions of two Si atoms in SAPO-34 when the negative charge in the framework is compensated by a Cu²⁺-TEPA organic complex occupying the cavity or by isolated Cu²⁺ cations located at four-, six- or eight-membered rings (4R, 6R, or 8R sites).

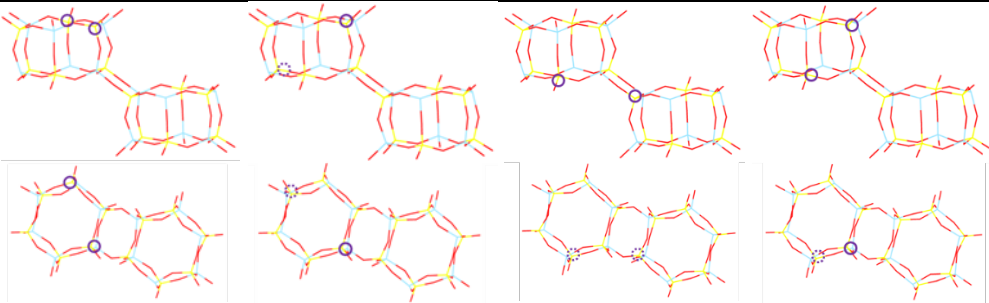
Si distribution	6RA	6RC	8R	4R
				
Cu ²⁺ -TEPA	0.0	2.3	0.1	8.9
Cu ²⁺ at 4R	39.8	43.6	41.5	15.3
Cu ²⁺ at 6R	0.0	16.9	14.2	18.1
Cu ²⁺ at 8R	35.2	39.2	14.6	34.1

Table S4. Calculated kinetic constants k_r for the non-catalyzed NO oxidation with O₂ following the mechanism reported by Maestri and Iglesia⁴ and for NO disproportionation following the pathway shown in Figure S10 at different T (in K). The apparent activation energy ΔG_{act} is calculated as the difference in Gibbs free energy between the highest point in the energy profile and the three separated reactant molecules, so that the entropy loss associated to formation of the reactants trimers is taken into account.

T (K)	298	373	473	623
$2\text{NO} + \text{O}_2 \rightarrow 2\text{NO}_2$	1.57×10^{-6}	7.2×10^{-6}	2.76×10^{-5}	1.01×10^{-4}
$3\text{NO} \rightarrow \text{N}_2\text{O} + \text{NO}_2$	1.34×10^{-11}	2.95×10^{-9}	2.88×10^{-7}	1.96×10^{-5}
$k_r(\text{oxidation})/k_r(\text{disproportionation})$	1.17×10^5	2.47×10^3	9.59×10^1	5.17×10^0

Table S5. DFT calculated interaction energies (in kJ mol⁻¹) of NO and NH₃ with Cu⁺ and Brønsted acid sites in the 6RA model of Cu-SAPO-34.

	Cu ⁺	Brønsted
NO	-113	-25
NH ₃	-124	-144

Table S6. DFT calculated vibrational frequencies in the 1650 - 1500 cm⁻¹ range for the relevant intermediate structures studied in this work.

	Cu-SAPO-34		Cu-SSZ-13		
Structure	6RA	6RC	6RA	6RB	6RC
6	1613	1616	1622	1618	1621
	1596	1597	1603	1601	1601
6'	1585			1575	
7	1619	1621	1626	1626	1624
	1562	1561	1565	1565	1572
7'	1511			1523	
9	1848	1852	1858	1861	1862
	1546	1543	1539	1541	1543
10	1669			1644	
	1507			1525	
11	1565			1568	
12	1672			1671	
	1619			1624	
	1563			1568	
13	1979			1972	
	1551			1555	
	1494			1494	

FIGURES

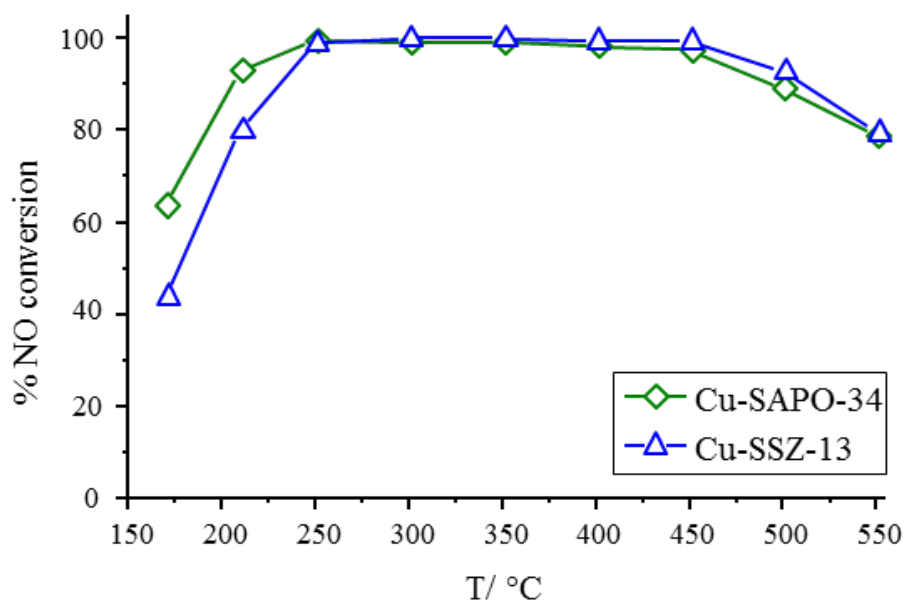


Figure S1. NO conversion in the NH_3 -SCR- NO_x reaction as a function of temperature for Cu-CHA catalysts prepared by one-pot synthesis. Reaction conditions: 500 ppm NO, 530 ppm NH_3 , 10 % O_2 , 5 % H_2O , N_2 as balance gas to a total flow of 300 ml/min, $450000 \text{ ml} \cdot \text{h}^{-1} \cdot \text{g}_{\text{cat}}^{-1}$. The two catalysts show very high activity from 200 °C to 550 °C, but especially in the 250 °C – 450 °C range where the NO conversion is over 99%.

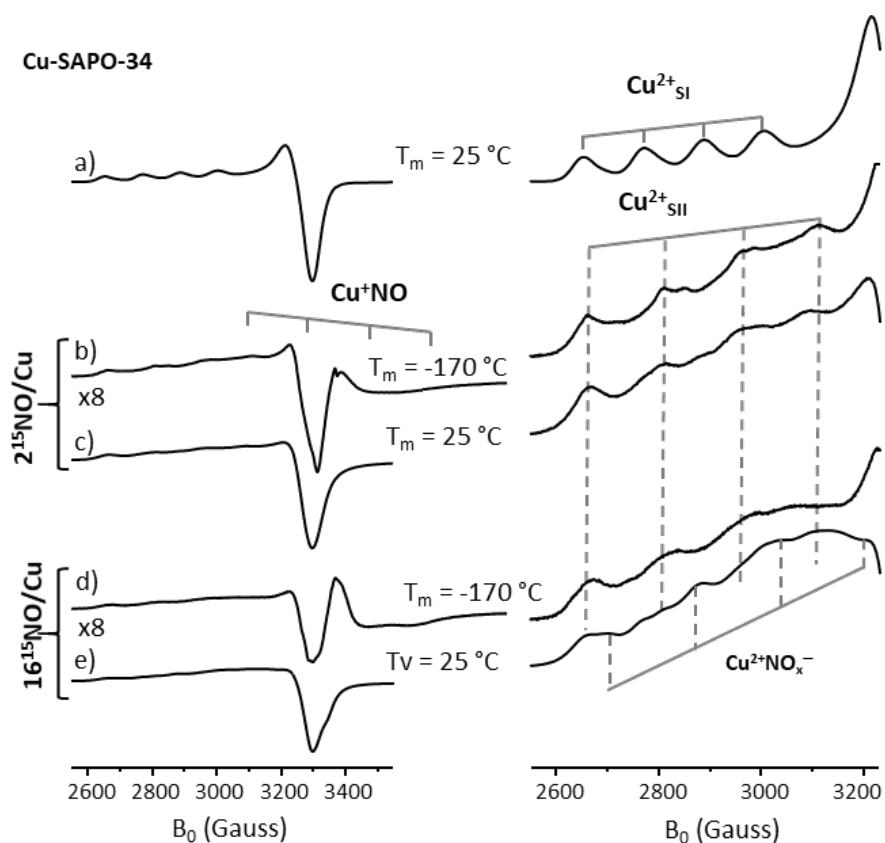


Figure S2. EPR spectra of Cu-SAPO-34 recorded after dehydration at 450 $^{\circ}\text{C}$ (a) and subsequent adsorption of 2 NO/Cu recorded at -170 $^{\circ}\text{C}$ (b) and 25 $^{\circ}\text{C}$ (c), and after adsorption of 16 NO/Cu recorded at -170 $^{\circ}\text{C}$ (d) followed by evacuation at 25 $^{\circ}\text{C}$ (e). Complete spectra are displayed on the left and magnification of the low-field hyperfine structure on the right side.

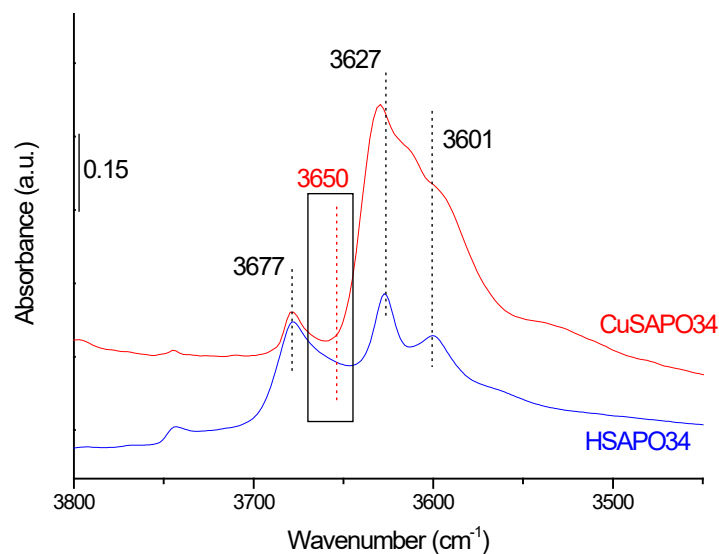


Figure S3. IR spectra in the νOH region of the Cu-SAPO-34 sample (red line) after activation in O_2 flow for 2h at 350°C followed by vacuum treatment at 150°C for 1h. Marked in a rectangle the IR region where the $\nu\text{Cu-OH}$ vibration should appear. The bands at 3677, 3631 and 3594 cm^{-1} correspond to silanol and Brönsted acid sites which are also present in the IR spectra of H-SAPO-34 (blue line).

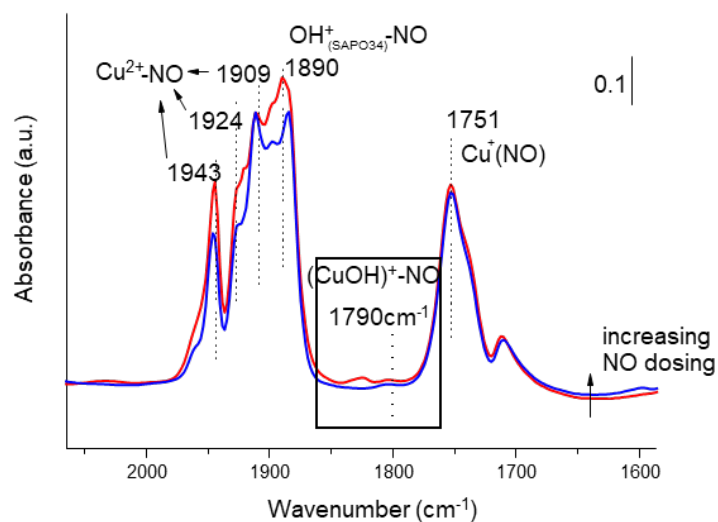


Figure S4. IR spectra of NO adsorption at -150°C on Cu-SAPO-34 sample at increasing NO dosing (0.2 and 0.5mbar). Sample activation: O_2 flow for 2h at 350°C followed by vacuum treatment at 150°C for 1h. Marked in a rectangle the IR region where Cu-OH interacting with NO should appear.

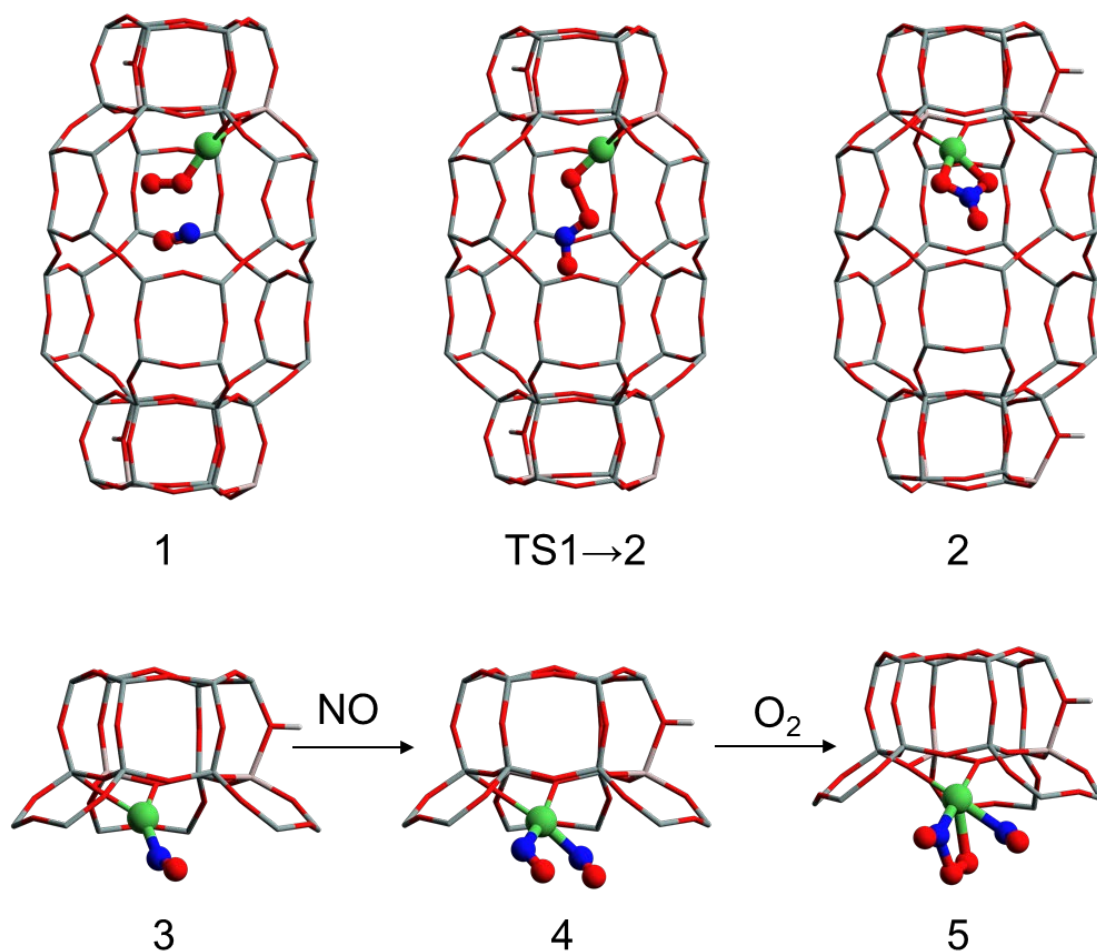


Figure S5. Optimized geometries of some NO and O₂ adsorption complexes (1, 3, 4 and 5), and of the structures involved in the direct formation of nitrate (2) from co-adsorbed NO+O₂ in Cu-SSZ-13. Al, O, Si, and H atoms in the framework depicted as gray, red, cyan and white sticks; Cu cations, O and N atoms in the reactant molecules depicted as green, red and blue balls.

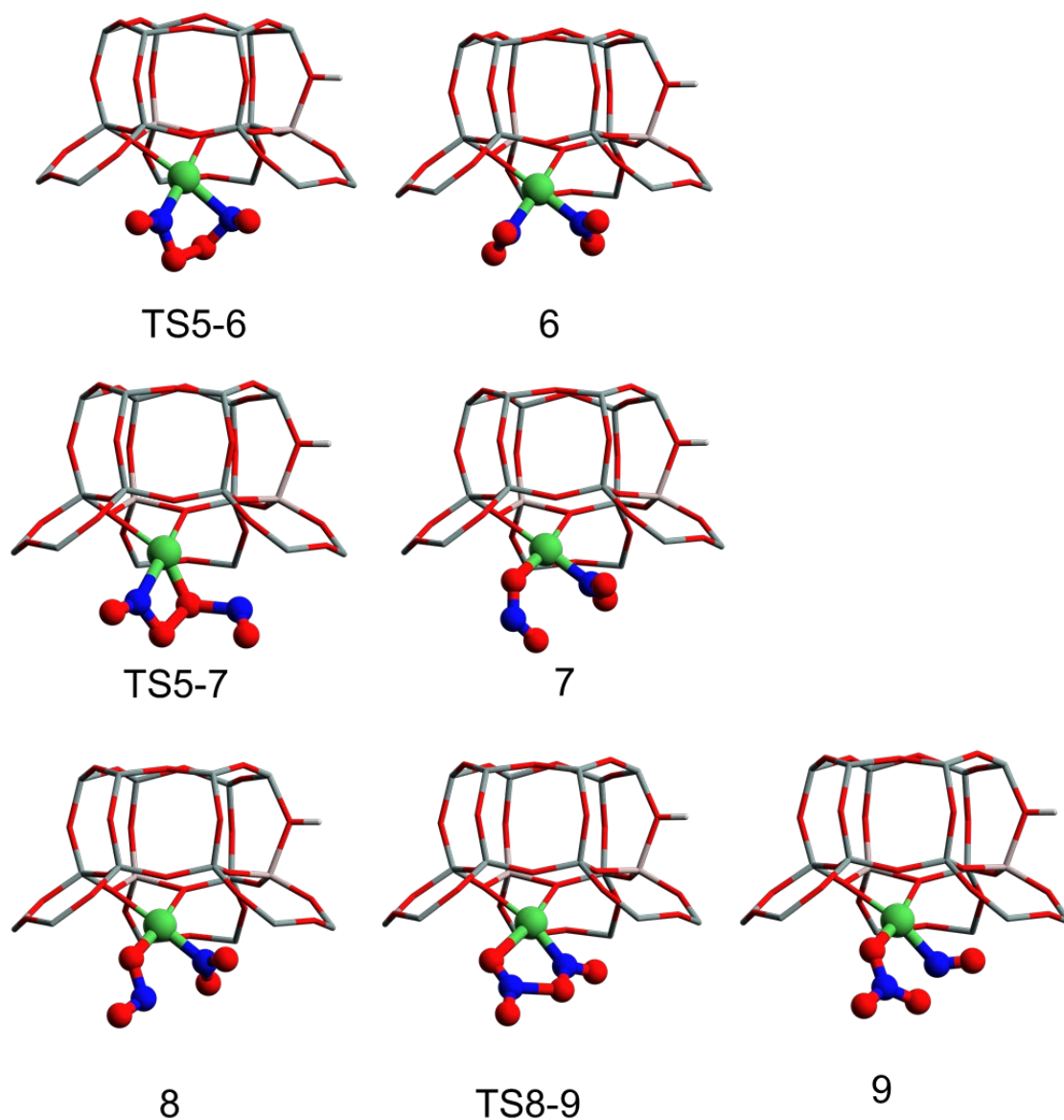


Figure S6. Optimized geometries of the structures involved in the formation of nitrites and nitrates from co-adsorbed $2\text{NO} + \text{O}_2$ (5) in Cu-SSZ-13. Al, O, Si, and H atoms in the framework depicted as gray, red, cyan and white sticks; Cu cations, O and N atoms in the reactant molecules depicted as green, red and blue balls.

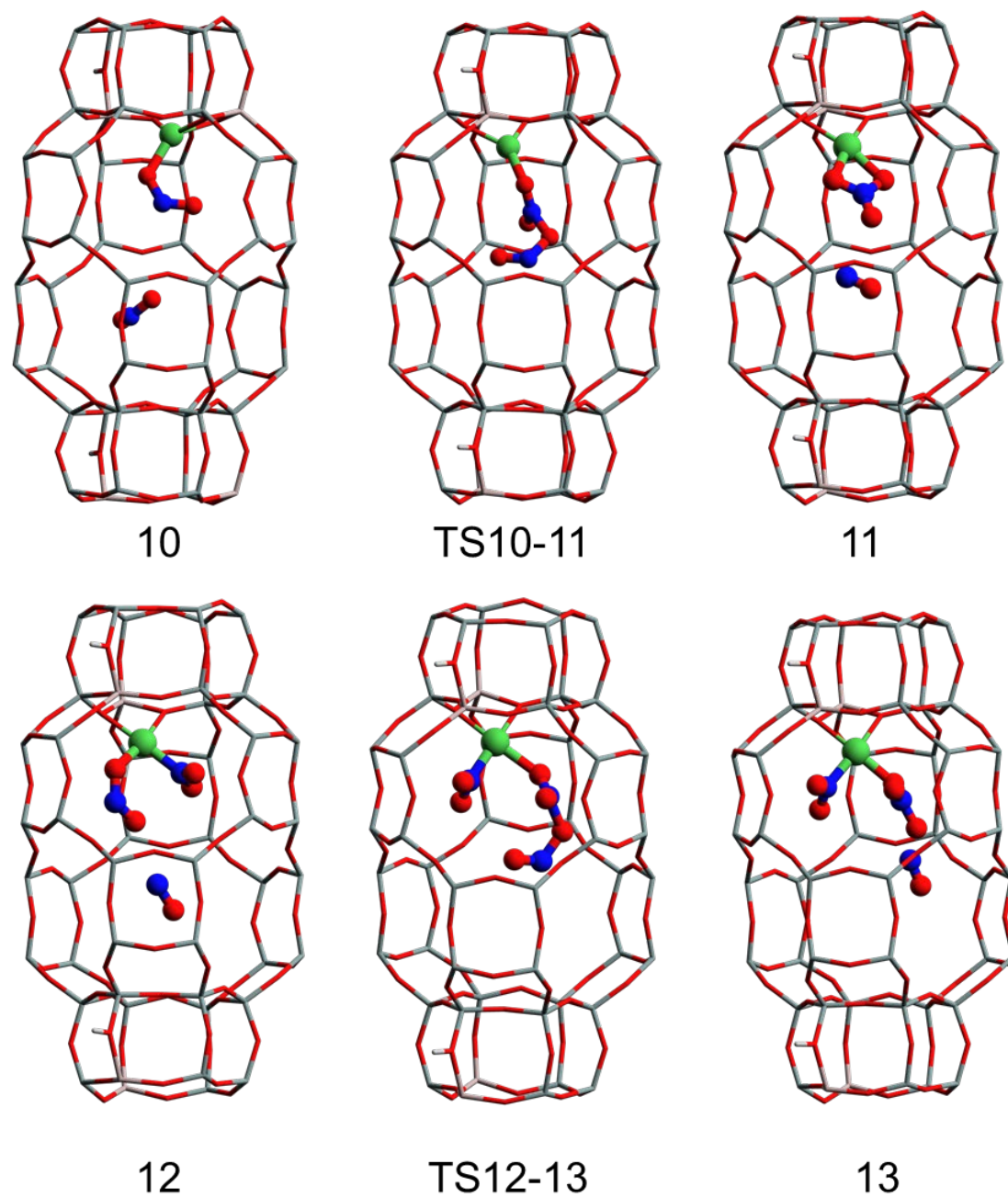


Figure S7. Optimized geometries of the structures involved in the formation of nitrates from NO_2 in Cu-SSZ-13. Al, O, Si, and H atoms in the framework depicted as gray, red, cyan and white sticks; Cu cations, O and N atoms in the reactant molecules depicted as green, red and blue balls.

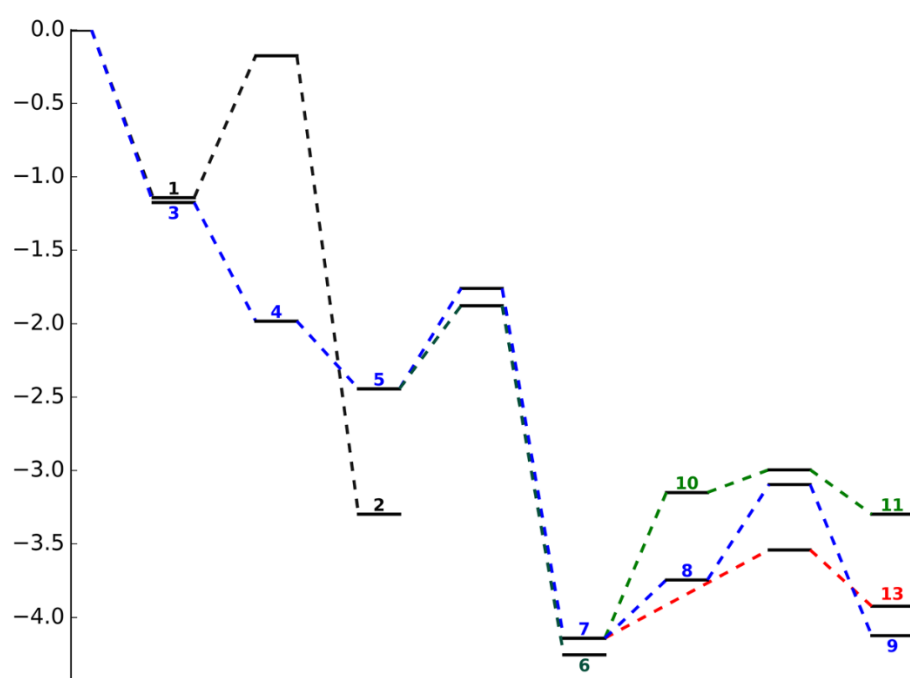


Figure S8. Calculated energy profile for all processes leading to formation of nitrites and nitrates from $\text{NO} + \text{O}_2$ and from NO_2 in Cu-SSZ-13 with Cu^+ in site 6RA. The optimized geometries of the structures involved are depicted in Figures S2-S4. Energies in eV.

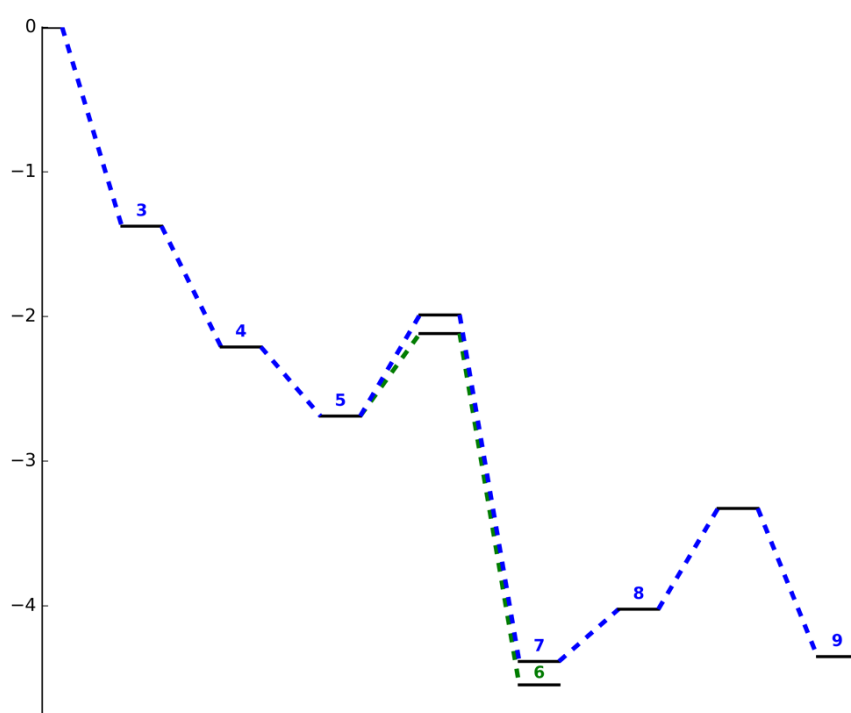


Figure S9. Calculated energy profile for all processes leading to formation of nitrites and nitrates from $\text{NO} + \text{O}_2$ in Cu-SAPO-34 with Cu^+ in site 6RC. Energies in eV.

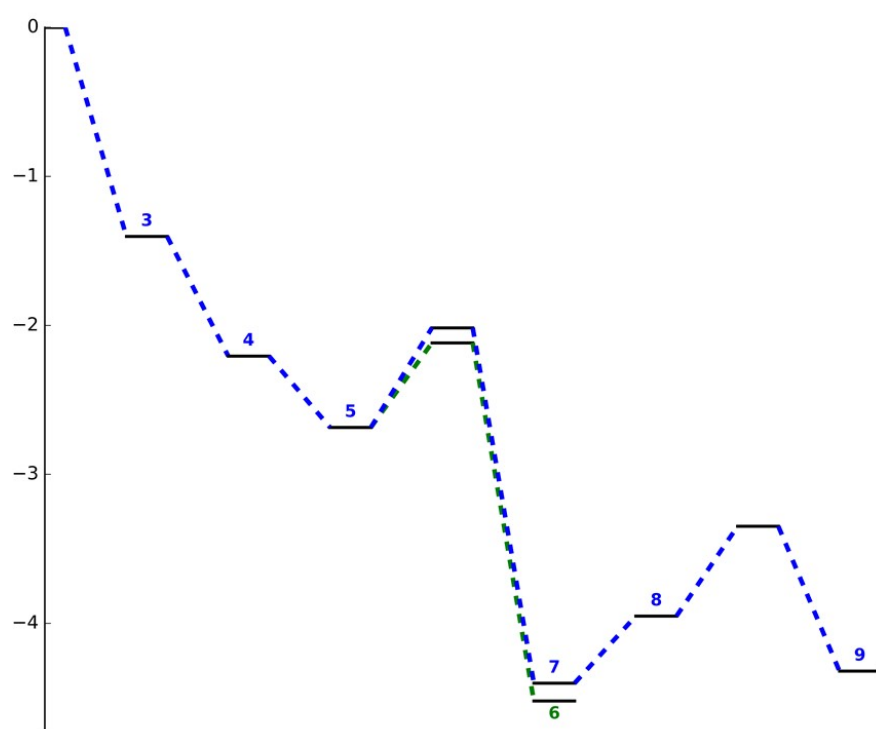


Figure S10. Calculated energy profile for all processes leading to formation of nitrites and nitrates from $\text{NO} + \text{O}_2$ in Cu-SSZ-13 with Cu^+ in site 6CR. Energies in eV.

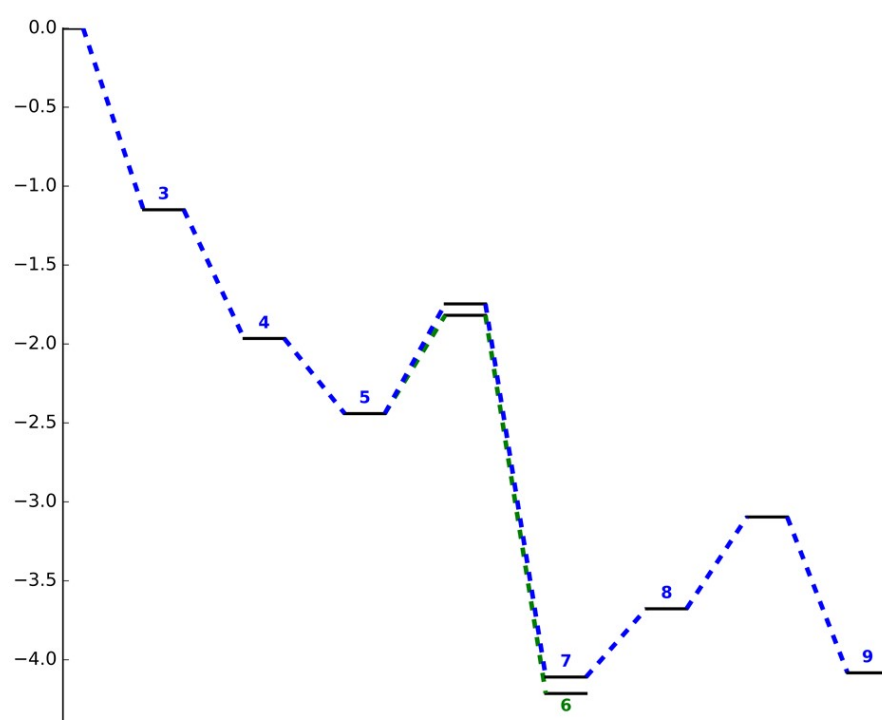


Figure S11. Calculated energy profile for all processes leading to formation of nitrites and nitrates from NO+O₂ in Cu-SSZ-13 with Cu⁺ in site 6RB. Energies in eV.

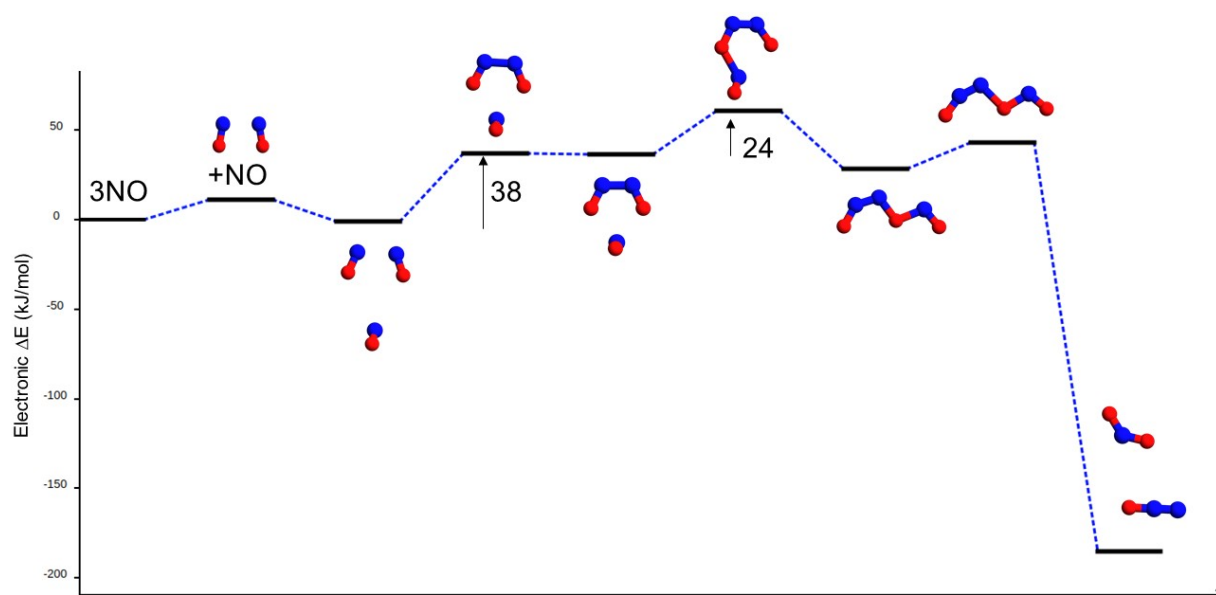


Figure S12. Optimized geometries and energy profile corresponding to the gas phase disproportionation of NO into N₂O and NO₂. Calculated at the B3LYP/cc-pVTZ level with Gaussian09 software in order to compare with the results from Maestri and Iglesia for the process $2\text{NO} + \text{O}_2 \rightarrow 2\text{NO}_2$. [4]

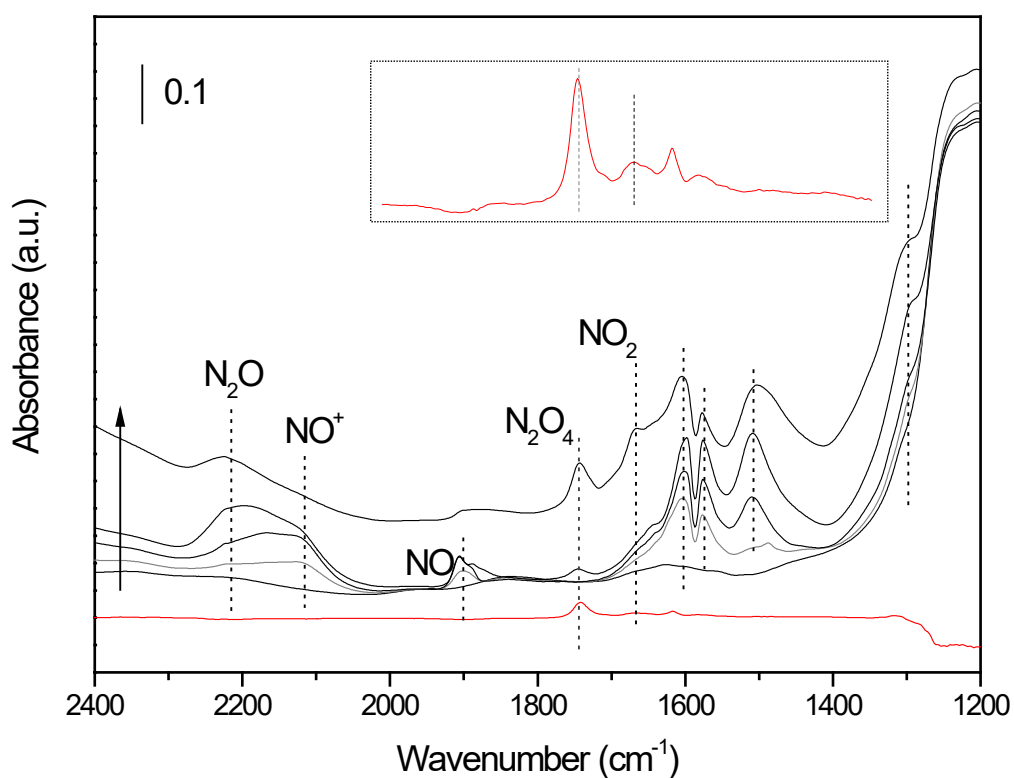


Figure S13. FTIR spectra of 2NO/5O₂/Cu adsorbed at 25°C on Cu-SAPO-34 (black line) and on H-SAPO-34 (red line) activated in O₂ at 350°C for 2h followed by vacuum at 150°C 1h. The inset shows a magnification of the 2000-1400 cm⁻¹ region of the spectrum obtained on H-SAPO-34, where the weak peaks corresponding to NO₂ and N₂O₄ can be observed. These spectra show that the contribution of the non-catalyzed NO oxidation to NO₂ in the absence of copper is very low.

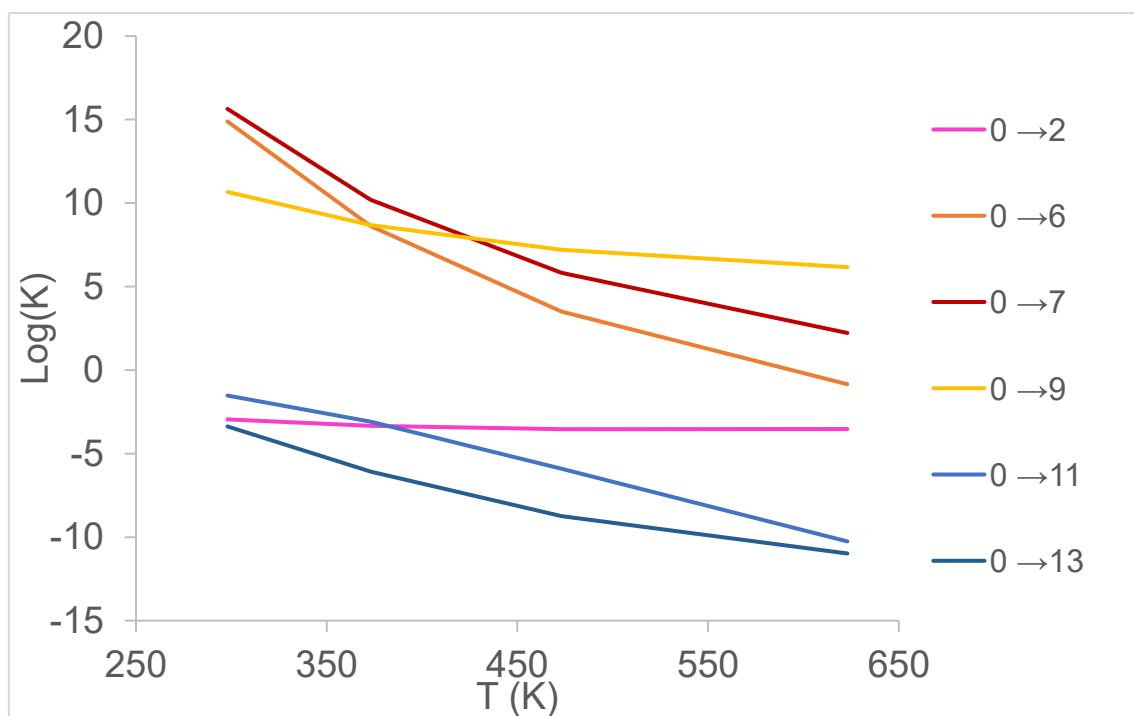


Figure S14. Plot of the logarithm of global rate constants for complete processes leading to formation of $\text{Cu}^{2+}\text{NO}_2^-$ and $\text{Cu}^{2+}\text{NO}_3^-$ from $\text{Cu}^+ + 2\text{NO} + \text{O}_2$ as a function of temperature on Cu-SSZ-13.

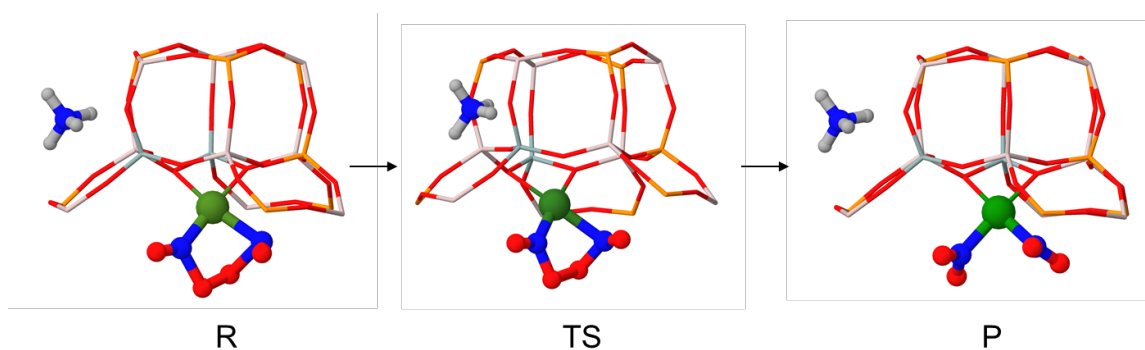


Figure S15. Optimized geometries of reactant R, transition state TS and product P for the oxidation of Cu^+ to Cu^{2+} according to the 5→6 pathway described in the manuscript, but in the presence of NH_4^+ adsorbed close to the active center, which is the most stable situation for adsorbed NH_3 . The calculated activation and reaction energies are 75 and -176 kJ mol^{-1} , respectively, not too different from the 57 and -178 kJ mol^{-1} calculated in the absence of NH_3 .

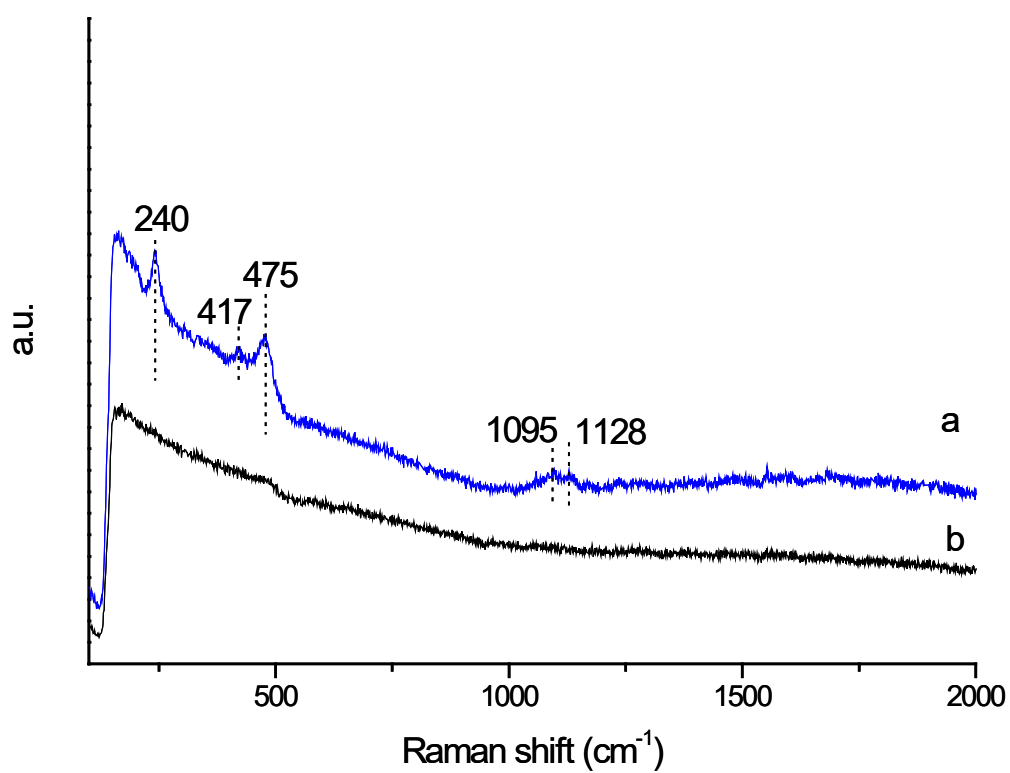


Figure S16. Raman spectra of Cu-SAPO-34 acquired at 25°C after O₂ preactivation at 230°C a) in O₂ flow and b) after flushing N₂.

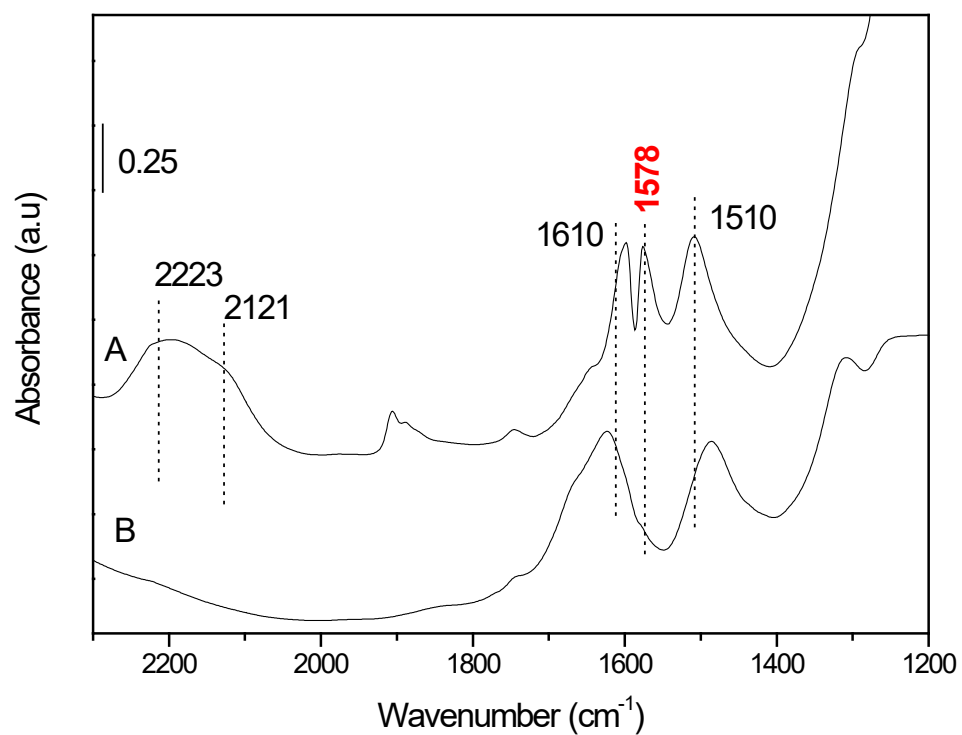


Figure S17. FTIR spectra of 2NO/5O₂/Cu adsorbed at 25°C on Cu-SAPO-34 (A) activated in O₂ at 350°C for 2h followed by vacuum at 150°C 1h and (B) activated at 450°C vacuum 1h.

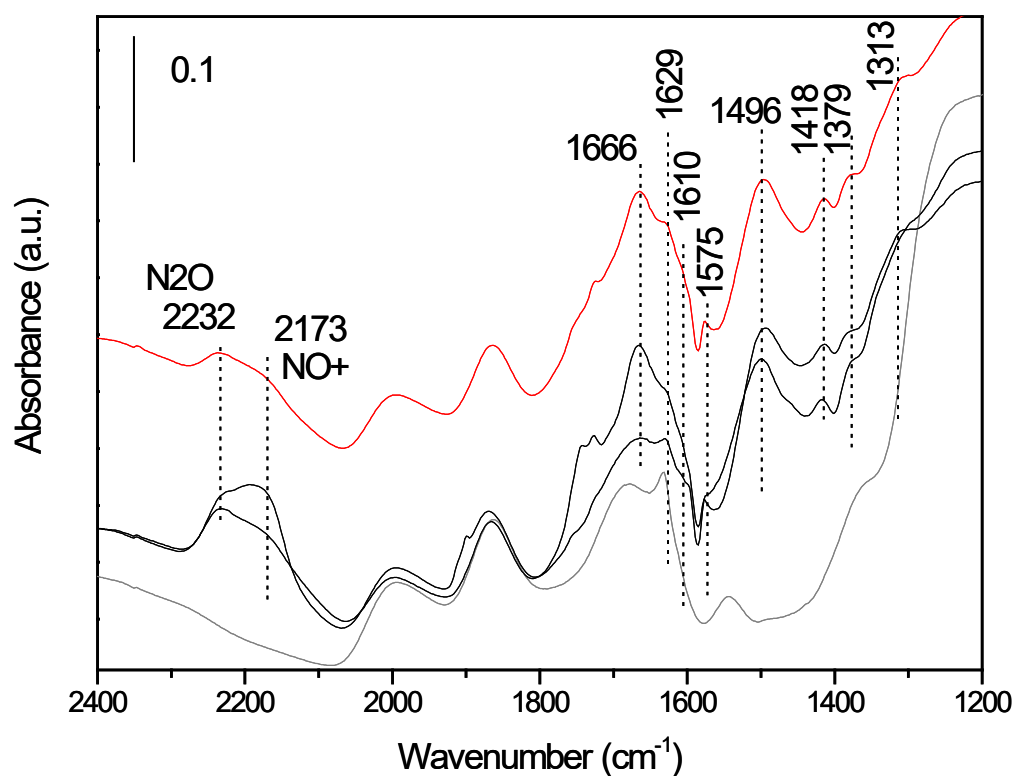


Figure S18. FTIR spectra of 2NO/5O₂/Cu adsorbed at 25°C on Cu-SSZ-13 at 1min and 62 min (black lines) and after increasing temperature to 150°C at 30 min (red line). Prior to the adsorption experiments the sample was activated in O₂ at 350°C for 2h followed by vacuum at 150°C 1h (grey line).

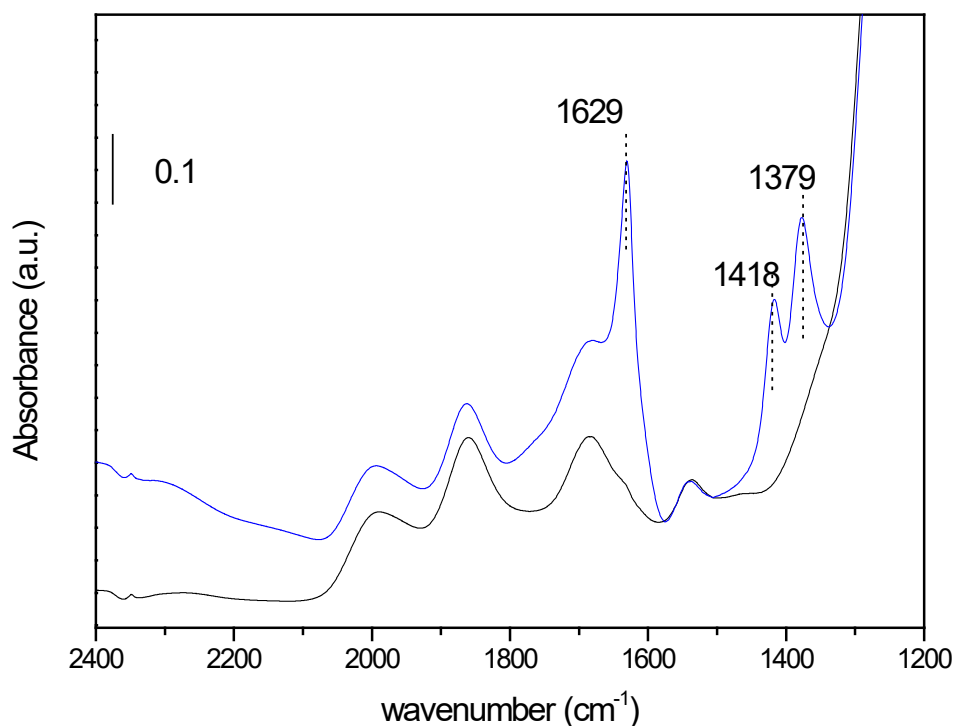


Figure S19. FTIR spectra of NO₂ adsorbed on the SSZ-13 sample. Black line corresponds to the sample before adsorption and blue line after adsorption. Prior to the adsorption experiments the sample was pre-activated in O₂ at 350°C for 2h followed by vacuum at 150°C 1h.

References

- [1] Frisch, M. J. et al. Gaussian 09, Revision C.01. Gaussian, Inc., Wallingford CT, (2009)
- [2] <http://www.iza-structure.org/databases/>
- [3] Cramer, C. J. *Essentials of Computational Chemistry: Theories and Models*. Wiley (2004).
- [4] Maestri, M.; Iglesia, E. , First-principles Theoretical Assessment of Catalysis by Confinement: NO–O₂ Reactions within Voids of Molecular Dimensions in Siliceous Crystalline Frameworks. *Phys. Chem. Chem. Phys.* **2018**, *20*, 15725–15735.